Type of contribution:
Editorial
▶ Research Paper
Case Study
Review Paper
Scientific Data
Report of Tech. Application

Mechanical Engineering for Society and Industry
Vol. 4, No. 1 (2024) pp 123-137
https://doi.org/10.31603/mesi.11724
e-issn. 2798-5245

# Influence of additive nano calcium carbonate ($CaCO_3$) on SAE 10W-30 engine oil: A study on thermophysical, rheological and performance

**Dany Ardymas Kurniawan**[1], **Poppy Puspitasari**[1,2*], **Ahmad Atif Fikri**[1], **Avita Ayu Permanasari**[1], **Jeefferie Abd. Razak**[3], **Diki Dwi Pramono**[1]

[1] Department of Mechanical and Industrial Engineering, Universitas Negeri Malang, Malang 65145, **Indonesia**
[2] Center of Advanced Material and Renewable Energy, Universitas Negeri Malang, Malang 65145, **Indonesia**
[3] Fakulti Teknologi dan Kejuruteraan Industri dan Pembuatan, Universiti Teknikal Malaysia Melaka, Durian Tunggal 76100, **Malaysia**
✉ poppy@um.ac.id

This article contributes to:

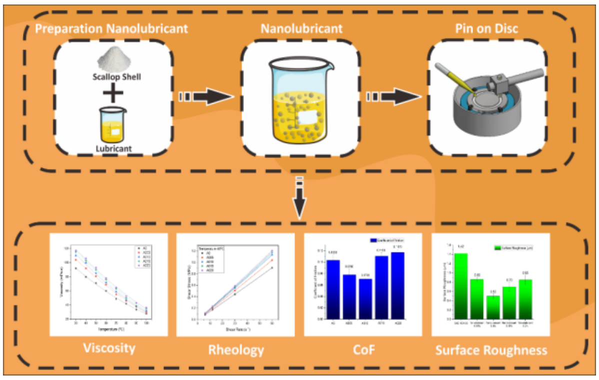


**Highlights:**

- Nano lubricants with calcium carbonate ($CaCO_3$) nanoparticles significantly improved wear and friction properties.
- A 0.1 wt% concentration of $CaCO_3$ nanoparticles provided the best wear reduction.
- The nano lubricants showed better thermal conductivity, density, and viscosity.

## Abstract

Researchers have used nanomaterials as additives in base oil to improve its specifications, especially to minimize wear and friction during its applications. In this study, calcium carbonate ($CaCO_3$) nanoparticles were selected as an additive to serve as a protective layer between components and anti-wear properties. In this study, calcium carbonate ($CaCO_3$) nanoparticles were selected as an additive to serve as a protective layer between components and anti-wear properties. Nano lubricant samples were prepared using mass variations of $CaCO_3$ and SAE 10W-30 base oil with concentrations of 0.05, 0.1, 0.15, and 0.2%, then homogenized. The nanolubricant samples obtained were analyzed for thermophysical, rheological properties and lubricant performance with the addition of nano $CaCO_3$ in improving the wear resistance of FC25 cast iron. The results of thermophysical and rheological properties analysis suggest that the nanolubricant has better tribological properties compared to base lubricants. The highest values of thermal conductivity, density, and viscosity (40 °C) are 0.139 W/m.K, 812.203 kg/m$^3$, and 106 mPa.s (40 °C). Meanwhile, the highest CoF, disc mass loss, and surface roughness of nanolubricant are 0.0706, 0.0037 grams, and 0.50 µm, respectively. These results indicate that the greatest wear-reducing agent is from the nanolubricant with the addition of $CaCO_3$ nanopowder additives at 0.1 wt% concentration. These results are expected significant insights into the advancement of nano technology-based lubricants in the future.

**Keywords:** Nanolubricant; Calcium carbonate; Thermophysical; Rheological; Wear

**Article info**
Submitted: 2024-07-04
Revised: 2024-07-26
Accepted: 2024-07-27



**Publisher**
Universitas Muhammadiyah Magelang

## 1. Introduction

Transportation is the main need in Indonesia as it supports daily activities. To address this demand, the automotive industry annually escalates production by 10% [1]. Consequently, lubricant has become a common need in the automotive industry since it significantly lowers friction and wear on essential components, ensuring maximum machine performance [2]. Friction and wear are the two central problems on some or all parts of the contacting surfaces, resulting in excessive energy loss [3]. Excellent lubrication reduces friction and energy loss by lowering the direct contact between the contacting surface [4]. In engines, lubricants function as vibration dampers, coolants, and dirt-transporting agents in internal combustion engines [5]. The improvement in the lubricant's performance and quality can be attained through the addition of additives [3].

Globally, lubricants contain less than 85% of base material in the form of petroleum [6]. The petroleum undergoes additional refining processes to yield mineral oil, which serves as the primary component for manufacturing lubricants. Generally, lubricants contain 90% of base oil, while the remaining 10% is in the form of additives [7]. The progression of lubricant involves the addition of an additive (nanoparticle) thus, its result is named nanolubricant. Nanolubricants have different physical and tribological properties that affect their performance compared to base oils [8]. Nanolubricant quality is influenced by several parameters, such as the variations in nanoparticle volume, shape and dimensions of nanoparticles, basic oil, as well concentration of nanoparticles [9]. The addition of nanoparticles accelerates the quality of basic oil, resulting in greater thermophysical properties.

In this study, nanoparticles $CaCO_3$ which originated from synthesized scallop shells in nano-sized powders were chosen as an additive because they have anti-wear and friction-reducing properties that are rarely known to many researchers [10], [11] and have many polymorphic structures that can be applied to industrial products [12]. The finished calcium carbonate nanoparticles have been added as an additive to 10W-30 base oil, the choice of base oil is because the viscosity of 10W-30 is widely used as a motor vehicle lubricant in tropical countries, especially Indonesia. As a lubricant additive, calcium carbonate reduces carbon deposition carbon and sulfur, which serve as the cleaning agent in the piston rings, pistons, and cylinders. The dispersed carbonate calcium nanoparticle on the basic oil forms the protective tribofilm that coats the contacting surfaces to lower the wear and enhance the performance of the lubrication [13]. The calcium carbonates contained in the oil lubricant maintain the required total base number (TBN) in the lubricant.

However, the long-term use of nanolubricant may result in stability issues on the nanolubricant due to the agglomeration induced by the high surface activities [2]. This occurrence inhibits the nanoparticle transfer from the base oil into the contacting surface, which forms the protecting layer. Consequently, to lower the agglomeration on nanolubricant, the dissolved particle concentration can be regulated [14]. In this study, the prepared nanolubricant sample was applied to the FC25 iron cast to examine its wear level. The FC25 iron cast is frequently used on the cylinder liner [9]. A cylinder liner is a crucial component of an engine as it facilitates piston movement, resulting in reciprocating piston movement [15], minimizing material damage, lowering fuel consumption, and elongating the component life of excellent lubrication [16].

Therefore, this study aims to identify the characteristics of $CaCO_3$ nanoparticles synthesized from the scallop shell, specifically for the additive on the SAE 10W-30 lubricant. The thermophysical and rheological properties of prepared nanolubricant with variations of CaCO3 nanoparticle addition (0.05%, 0.1%, 0.15%, dan 0.2% wt) were examined. The SAE 10W-30 added with $CaCO_3$ nanoparticle variations was applied on the FC25 iron cast to identify its wear resistance using the pin-on-disc machine.

# 2. Methods

## 2.1. Material

This study used SAE 10W-30 lubricant and calcium carbonate powder obtained from synthesized scallop shells. The details of the materials being used are summarized in **Table 1**. The properties of the SAE 10W-30 lubricant brand Shell Advance brand are listed in **Table 2**. Meanwhile, the material used for the wear and surface roughness test was the FC25 iron cast. The information related to the materials being used in this study is briefly described in **Table 3**.

**Table 1.** The material used for nanolubricant preparation

| Sample Name | Category | Function | Product |
|---|---|---|---|
| SAE 10W-30 | Dispersed Phase | Lubricant Oil | Shell Advance |
| $CaCO_3$ | Dispersion Medium | Nanoparticle | Synthesis Scallop Shell |

**Table 2.** Properties of lubricant 10W-30 [17]

| Parameters | Values |
|---|---|
| SAE viscosity grade | 10W-30 |
| Density at 15 °C (kg/m$^3$) | 881 |
| Kinematic viscosity at 40 °C (cSt) | 75.1 |
| Kinematic viscosity at 100 °C (cSt) | 11.5 |
| Dynamic viscosity at -25 °C (mPa.s) | 6700 |
| Viscosity index | 147 |

**Table 3.** Chemical compositions of grey cast iron FC25 [18]

| Conditions | Composition (%) | | | | | |
|---|---|---|---|---|---|---|
| | C | Mn | Si | P | S | Fe |
| Min | 2.44 | 0.39 | 1.83 | 0.15 | - | Balance |
| Max | 3.02 | 0.52 | 2.03 | 0.30 | 0.15 | |

## 2.2. Nanolubricant Preparation

The nanolubricant samples were prepared using variations of $CaCO_3$ mass and SAE 10W-30 basic lubricant with concentrations of 0.05, 0.1, 0.15, and 0.2%. The use of these variations refers to the research of Jose, et al. that adding $CaCO_3$ to PAO8 oil can reduce the acidity between up to 60% [19]. so that these variations are used in this study to reduce the wear value to the maximum. The procedures for nanolubricant preparation are illustrated in Figure 1. The comprehensive information on the samples employed can be found in Table 4. Following several calculations, 200 ml of basic lubricant was prepared. The $CaCO_3$ nanoparticle powder at mass variations of 0.05, 0.1, 0.15, and 0.2% was prepared. Then, each sample was stirred using a magnetic stirrer at 1250 rpm speed for 20 minutes at room temperature. Further, a sonication process was carried out using an ultrasonic homogenizer for 30 minutes to obtain a homogeneous mixture of $CaCO_3$ and SAE 10W-30 lubricant. Homogenization aims to homogenize the particle size in order to maintain the stability of the mixture [20]. After this process, the prepared nanolubricant samples were further examined.

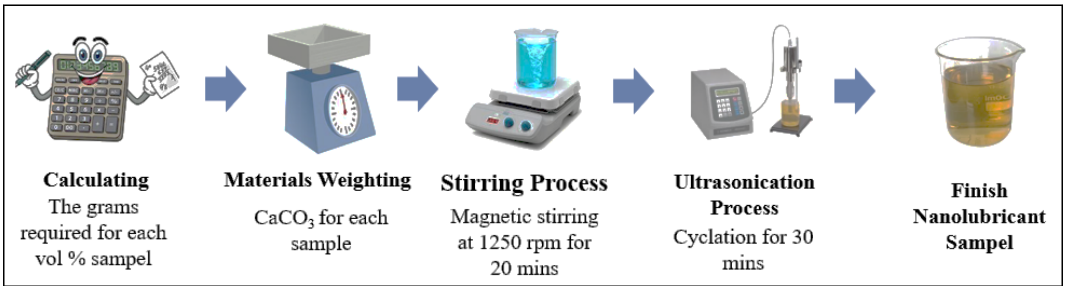


**Figure 1.** Procedures of nanolubricant preparation

**Table 4.** Detail of samples used in the study

| Base Oil | Concentration of Nanoparticles $CaCO_3$ (wt %) | Samples Code |
|---|---|---|
| SAE 10W-30 | - | A0 |
| | 0.05% | A005 |
| | 0.1% | A010 |
| | 0.15% | A015 |
| | 0.2% | A020 |

## 2.3. Material Characterization

The characteristics of $CaCO_3$ nanoparticles originating from scallop shell waste were analyzed using X-ray Diffraction (XRD) type E'xpret Pro, specifically to identify its crystal structure, crystallite size, and phase. Besides, the samples were also characterized using Scanning Electron Microscopy (SEM) type Inspect-S50 for the identification of the $CaCO_3$ nanoparticle's morphology. Another characterization using Fourier Transform Infra-Red (FTIR) type Irprestige 21 was also performed to identify the compounds, functional groups, and impurities within the $CaCO_3$ nanoparticle powder from the scallop shell waste.

## 2.4. Thermophysical Properties Test

The thermophysical test was conducted to determine the thermal conductivity of the samples using the thermal properties analyzer KD2 Pro illustrated in Figure 2a. In specific, this test was carried out to identify the heat transfer value through conduction. The viscosity of the nanolubricant was tested using the NDJ-8S Viscometer illustrated in Figure 2b. Meanwhile, the density was tested using an analytical digital balance by dividing the mass by its volume to determine the density of the nanolubricant. Further, sedimentation was assessed after the nanolubricant solution was set aside for 30 days. The sedimentation results were photographed to examine the precipitation in the solution.


**Figure 2.** Thermophysical properties testing equipment: (a) Analyzer KD2 Pro; (b) NDJ-8S Viscometer

## 2.5. Rheology Characterization

The rheological properties are employed to ascertain the flow of the nanolubricant, investigating the correlation between shear rate and stress. The shear rate and shear stress analysis required the viscosity results. in rheology testing of lubricants conducted at temperatures of 40 °C and 100 °C [21]. The shear rate was calculated using Eq. (1) [22], while the shear stress calculation was performed using Eq. (1).

$$\gamma = \frac{2\omega {R_c}^2 {R_b}^2}{x^2({R_c}^2 - {R_b}^2)} \quad (1)$$

in which γ means the shear rate (1/s), ω is the angular velocity (rad/sec), Rc is the contained radius (cm), Rb represents the rotor radius (cm), X represents the radius at which the shear rate was computed (cm). Meanwhile, to calculate the shear stress value, we can use Eq. (2) [22].

$$\tau = \mu \times \gamma \quad (2)$$

where τ is the shear stress (mPa.s), µ is the dynamic viscosity (kg/m.s), γ is the shear rate (1/s).

## 2.6. Experimental Setup

**Table 5.** Specification materials of pin on disc test

| Category | Materials | Hardness (HV) |
|---|---|---|
| Pin | Stainless Steel | 265.1 |
| Disc | Grey Cast Iron FC25 | 194.7 |

**Table 6.** Parameters of pin on disc testing [23]

| Parameters | Value |
|---|---|
| Force (N) | 20 |
| Sliding Speed (m/s) | 0.1 |
| Sliding Distance (m) | 1000 |
| Track Diameter (mm) | 30 |
| Temperature (°C) | 23 |
| Pin Diameter (mm) | 6 |
| Disc Diameter (mm) | 60 |

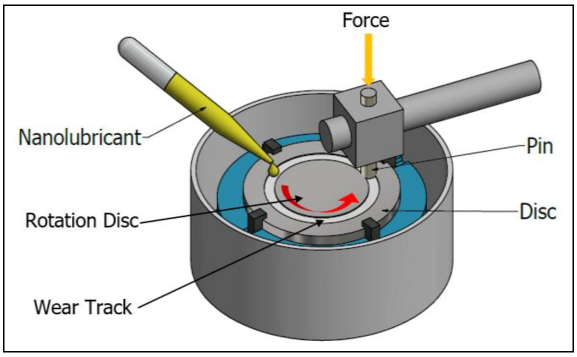


**Figure 3.** Schematic of pin on disc test

The performance of the nanolubricant with $CaCO_3$ nanopowder additive was analyzed using a wear test through a pin on disc tribometer from Ducom Instruments. The materials used in this wear test are shown in **Table 5** obtained from the test results in the mechanical engineering laboratory. The use of stainless-steel material for the pin was assumed to be the material for the piston rings. Meanwhile, the use of FC25 gray cast iron material was assumed to be in accordance with the material in the cylinder liner on the engine.

The wear test was conducted following the ASTM G99 standards, and referring to the research of Kurre, et al. with parameters summarized in **Table 6**. Meanwhile, the pin on disc test is illustrated in **Figure 3**. Besides, the surface structure of the obtained pin-on-disc test was observed through the photo taken from a microscope.

# 3. Results and Discussion

## 3.1. Additive Characterization

Scanning Electron Microscopy (SEM) was used to examine the morphology of $CaCO_3$ powder from the synthesized scallop shell's waste. The SEM results are illustrated in **Figure 4**, suggesting the spherical shape and uniform size of the calcium carbonate synthesized from the scallop's shell [24]–[26]. The results also indicate the presence of agglomeration caused by numerous factors, such as sintering temperature, sintering time, uneven demolition, and the period of demolition [26]. For resolving the agglomeration on the calcium carbonate added into the basic lubricant, further processes using the magnetic stirrer and sonication are required to produce a more stable nanolubricant [27].

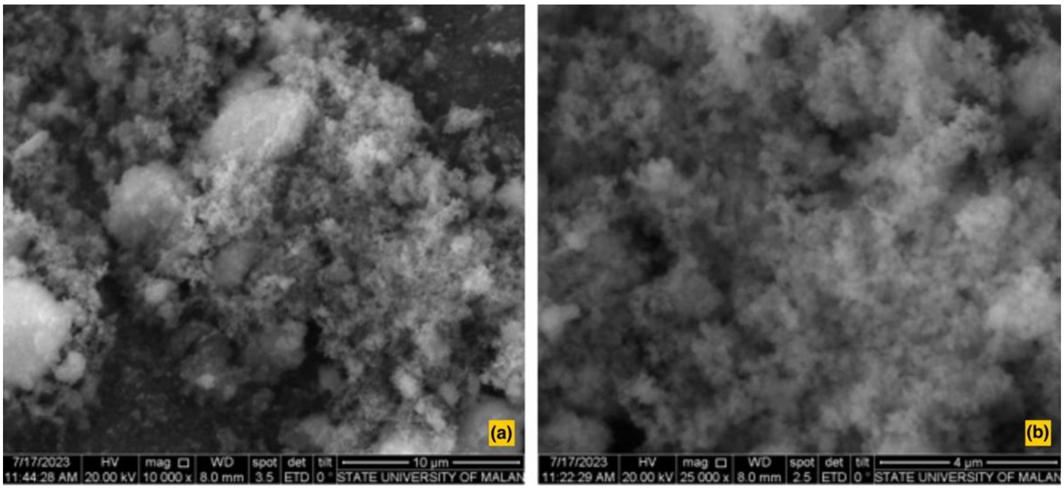


**Figure 4.** Scanning electron microscopy of calcium carbonate additive, (a) Magnification 50.000x, (b) Magnification 100.000x

X-ray diffraction (XRD) characterization was performed to identify the properties of $CaCO_3$ material synthesized from the scallop shell waste, including its phase, crystal structure, and crystallite size [28]. The crystallite size of $CaCO_3$ material synthesized from the scallop shell waste was calculated using the Scherrer formula [29], with Eq. (3).

$$d = \frac{K\,\lambda}{\beta\cos\theta} \tag{3}$$

Where, d: Crystallite diameter; K: 0.9; $\lambda$: Wavelength = 1.5406 Å. and $\beta$ : Full-Width Half Maximum (FWHM).

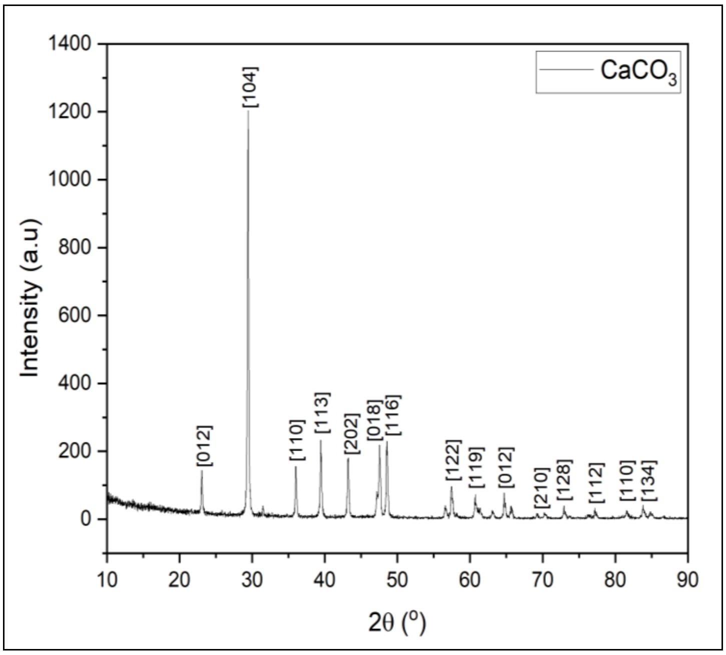


**Figure 5.** XRD analysis of calcium carbonate

The crystallite size of $CaCO_3$ powder is 52.18 nm. Additionally, according to the XRD results illustrated in **Figure 5**, the scallop shell's powder sample has a single phase with calcite symmetry crystals indicated from the highest peak of 1194.07 at 2θ=29.4554° and trigonal crystal (hexagonal axes) [24].

Through the FTIR analysis, the functional group of calcium carbonate was examined. The FTIR results for $CaCO_3$ are presented in **Figure 6**, showing a sharp peak at 2916.36 cm$^{-1}$ and 2848.86 cm$^{-1}$, indicating C-H bending vibration due to the

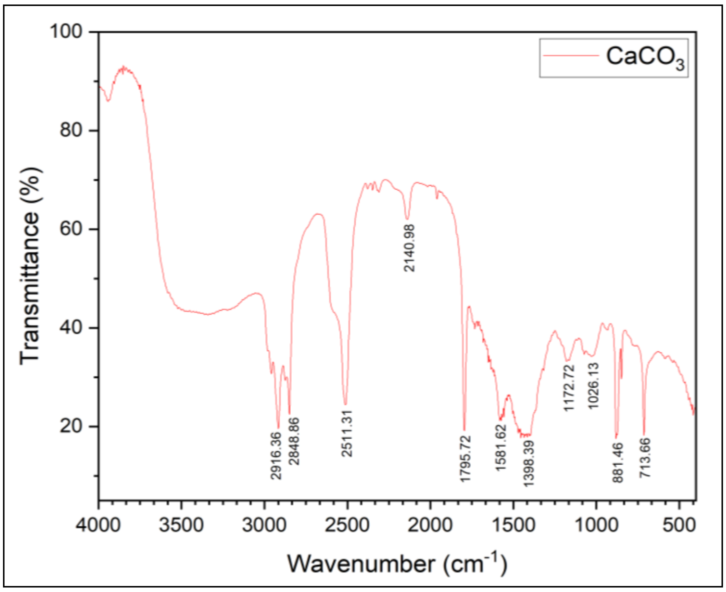


**Figure 6.** FTIR of calcium carbonate additive

organic layer from the amino acid from the scallop shell [30]. Besides, the absorption peak at 2511.31 cm$^{-1}$ shows the C-H stretching vibration, suggesting the existence of different calcium carbonate bonds [31], [32]. Meanwhile, the peak at 1398.39 cm-1 represents the characteristics of calcium carbonate of scallop shell [33]. The absorption peak of pure calcium carbonate was detected at 881.46 cm$^{-1}$ and 713.66 cm$^{-1}$, suggesting its calcite characteristic [33], [34].

## 3.2. Thermophysical Properties of Nanolubricant

### 3.2.1. Thermal Conductivity of Nanolubricant

Thermal conductivity represents the heat transfer ability of a material. The thermal conductivity of nano-sized particles presents a significant influence on the nanolubricant conductivity [35]. **Figure 7** presents the thermal conductivity of the base oil and the nanolubricant with the addition of a $CaCO_3$ nanoparticle. The obtained data suggested 0.137 W/m.K and 0.139 W/m.K thermal conductivity of the base oil and the lubricant added with the $CaCO_3$, respectively.

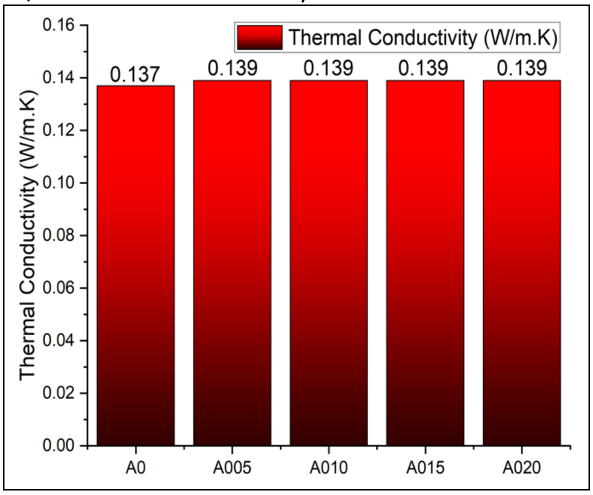


**Figure 7.** Thermal conductivity of nanolubricant

This increase in thermal conductivity is caused by the addition of inorganic nanomaterial [36], [37]. Further, the different addition of $CaCO_3$ nanoparticles shows no significantly different increase in thermal conductivity due to a number of factors, including the non-homogeneous particle size [38], change of temperature [39], particle size of $CaCO_3$ synthesized from the shell waste [40], and nanoparticle conductivity [41]. In addition, the addition of nanoparticles will produce brownian motion that can increase the heat transfer rate of the nanolubricant [42].

### 3.2.2. Density of Nanolubricant

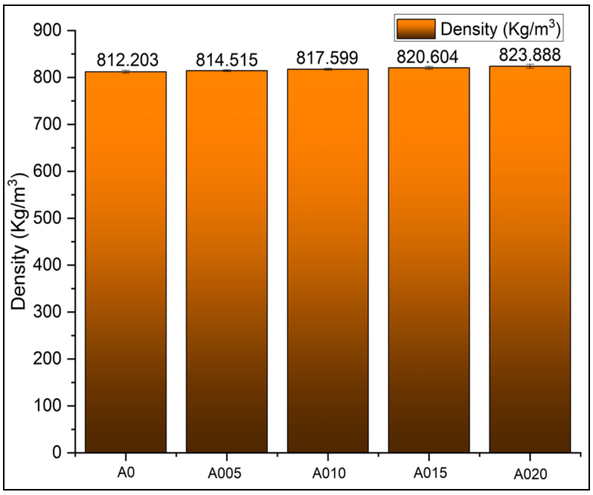


**Figure 8.** Density of nanolubricant

We identified different densities from each sample of nanolubricant. The increase in density is directly proportional to the higher composition of nanoparticles [43]. **Figure 8** also presents the results of the density test from the basic lubricant and nanolubricant with variations of $CaCO_3$ nanoparticles. The highest density of 823.888 kg/m$^3$ is observed from the nanolubricant with a 0.2% addition of $CaCO_3$. In contrast, the lowest density of 812.203 kg/m$^3$ is from the basic oil. The nanoparticle addition on base oil is directly proportional to the higher density [44], [45].

### 3.2.3. Viscosity of Nanolubricant

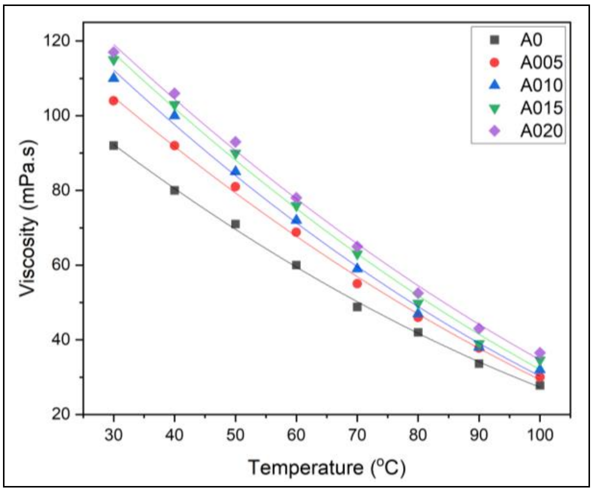


**Figure 9.** Viscosity of nanolubricant

**Figure 9** shows the results of viscosity examination from base lubricant and nanolubricant with variation addition of $CaCO_3$. **Figure 9** shows the highest viscosity from the nanolubricant with a 0.2% addition of $CaCO_3$ in comparison to the base oil. At 40 °C and 100 °C temperatures, the sample has 106 and 36.5 mPa.s, density. This finding signifies that high temperature correlates with low viscosity, which heads closer to the base oil [46] due to the lower Van Der Waals force among the molecules [47]. This viscosity value further impacts the rheology and nanolubricant features [48].

### 3.2.4. Sedimentation of Nanolubricant

The nanolubricant stability was observed using the sedimentation method. The nano lubricant's stability highly relies on the features of suspended particles and base oil [49]. **Figure 10** suggests the results of observation on the base oils and lubricants sedimentation at observation periods of 0, 10, 20, and 30 days. The results obtained showed that samples (b-e) had sedimentation on 10 days, as shown by the white sediment on the base of nanolubricant from the dried scallop shell powder, which was not dispersed properly on the base oil. Further, the same results were also identified on the 20 and 30 days of sedimentation. Several factors that affect the nano lubricants' stability include the nanoparticles concentration, use of surfactant, types of nanoparticle, and particle size [50]. It should be noted that the sedimentation that occurs in nanolubricants can be caused by gravity when nanoparticles are mixed in the base oil. Safril, et.al. also showed that the first day there was no sedimentation and after 30 days sedimentation occurred in a limited manner [51].

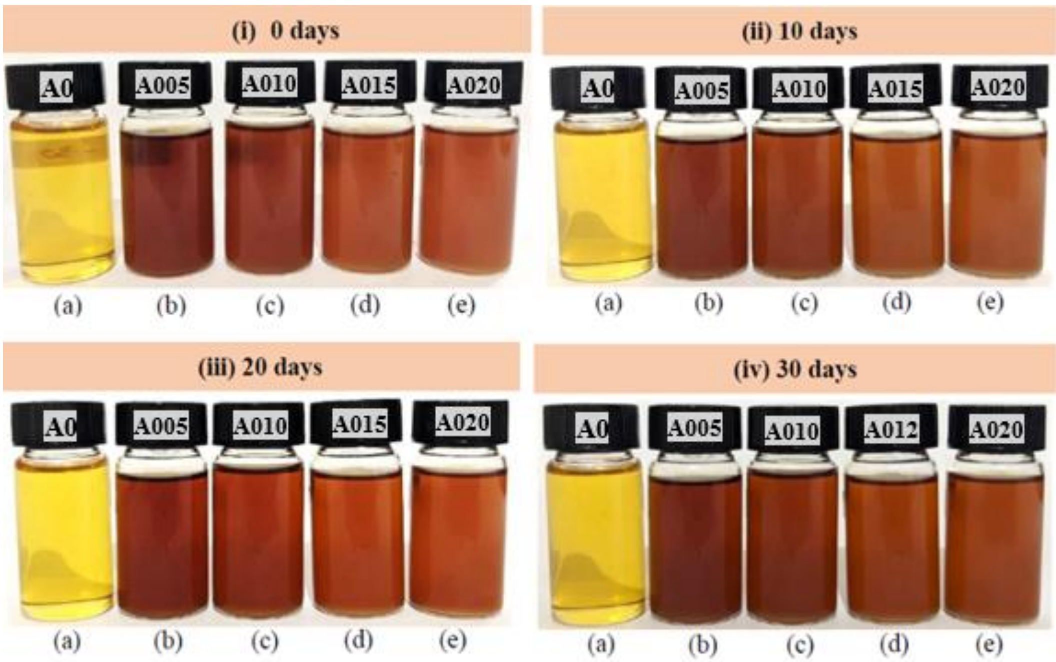


**Figure 10.** Visual observation of nanolubricant sedimentation

## 3.3. Rheological Behavior of Nanolubricant

The rheological property on nanolubricant represents the correlation between shear rate and shear stress. The calculation of rheology properties relies heavily on viscosity. The obtained rheology properties are presented in **Figure 11**, showing the comparison between the shear rate and shear stress on the base lubricant and nanolubricant added with $CaCO_3$ nanoparticle. At 40 °C and 100 °C temperature, a linear correlation between the shear rate and shear stress on SAE 10W-

30 and nanolubricant is observed. Thus, the SAE 10W-30 and nanolubricant with $CaCO_3$ nanoparticles have Newtonian flow [52]. Further, at 30 °C, the nanolubricant with nanoparticles experiences slight curve transformation, which is caused by the different structure of the base lubricant due to its broken molecule, resulting in the nanoparticle as the interface correlating the layers of oil [53].

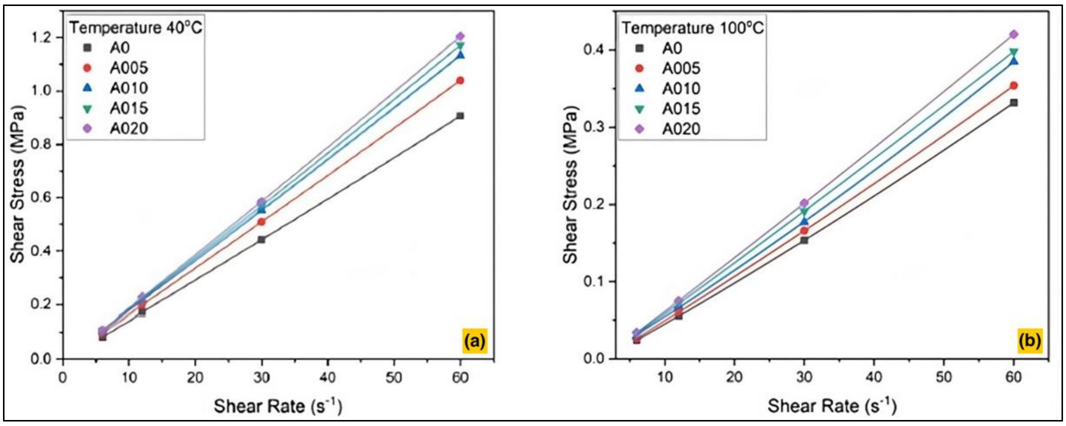


**Figure 11.** Rheology of nanolubricant for shear rate versus shear stress: (a) Temperature 40 °C; (b) Temperature 100 °C

## 3.4. Evaluation Performance of Nanolubricant

### 3.4.1. Wear and Friction

**Figure 12** presents the effect of $CaCO_3$ lubricant addition on the coefficient of friction (COF) and mass loss. The results of the COF test are shown in **Figure 12a**, signifying the maximum results of 0.117 obtained from nanolubricant with 0.2 wt% of $CaCO_3$ that enhance the COF of the base lubricant. Meanwhile, the lowest COF (0.0706) was garnered from the nanolubricant with the addition of 0.1 wt% $CaCO_3$. The decrease in the COF value is due to the higher viscosity of the nanolubricant, along with the addition of nanoparticles that forms a thin layer of tribofilm [54]. The decrease of COF is only found on the sample with 0.1 wt% of nanoparticle since the nanoparticle fills the gap between the surface maximumly, lowering the friction [55]. **Figure 12b** shows the mass loss from the disc after the pin-on-disc test. These results indicate that the highest mass loss (0.011 gram) is in the base lubricant. While the lowest mass loss occurs in nanolubricant (0.0037 gram) is found on the nanolubricant with the addition of 0.1 wt%. In summary, the mass loss relies on the COF, with the lower the COF reduces the mass loss value and vice versa. The lower coefficient of friction is caused by the addition of nanoparticles to the base lubricant [56].

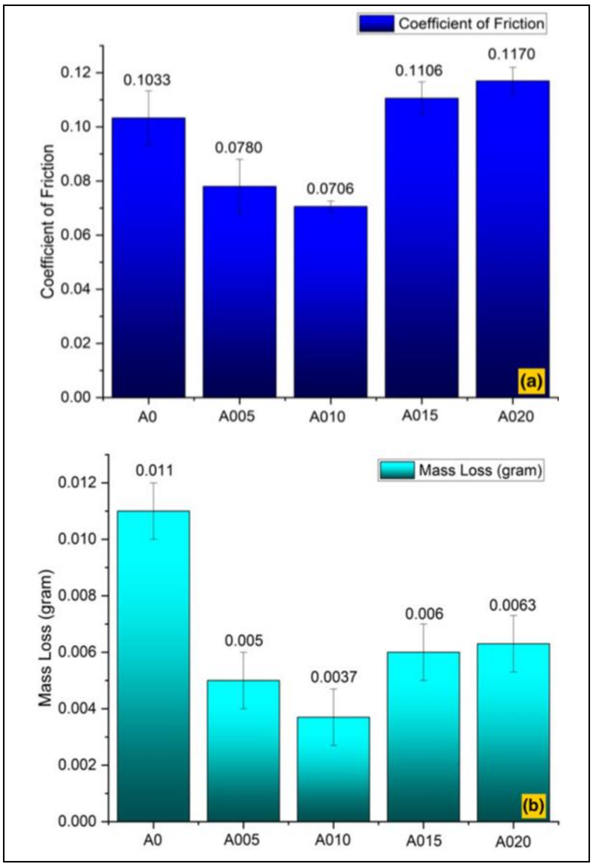


**Figure 12.** Nanolubricant test result on: (a) Coefficient of friction; (b) Mass loss

### 3.4.2. Surface Roughness

**Figure 13** presents the results of the surface roughness test from the FC25 iron cast after the pin-on-disc test on the wear track area. The results showed that the highest surface roughness (1.42 µm) is observed on the base oil sample. Meanwhile, the lowest roughness occurs in nanolubricant sample with the addition of 0.1 wt% $CaCO_3$. The nanoparticles' addition into base oil can reduce friction effectively, in comparison to the use of base oil without addition of the nanoparticles [57].

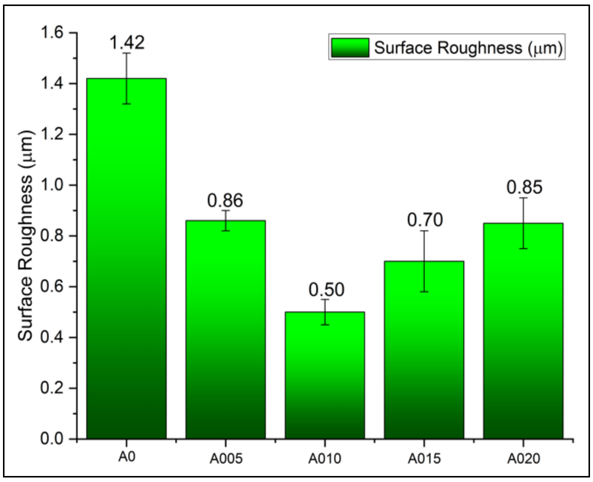


**Figure 13.** Surface roughness for all nanolubricant samples

However, the excessive addition of nanoparticles exceeding the maximum limit also decreases the wear rate caused by the formation of aggregate [58].

## 3.5. Analysis of Worn Surface

### 3.5.1. Macro Structure

The worn disc surface was analyzed through macro photos using an optical microscope to identify its type of wear after the pin ondisc test. **Figure 14a** shows the morphology of the disc surface from wear testing in dry conditions with delamination wear and parallel grooves in the direction of friction [59]. **Figure 14b-Figure 14f** shows the surface morphology with base lubricants and nanolubricant with the addition of $CaCO_3$ nanoparticle mass variations. The results suggest there are precise and similar grooves in the direction of friction, thus indicating wear of the abrasive and adhesive [54]. Additionally, the obtained surface morphology from basic lubricants and nanolubricant is smoother compared to dry conditions without lubricants. This occurrence is caused by the smoothing phenomenon [60].

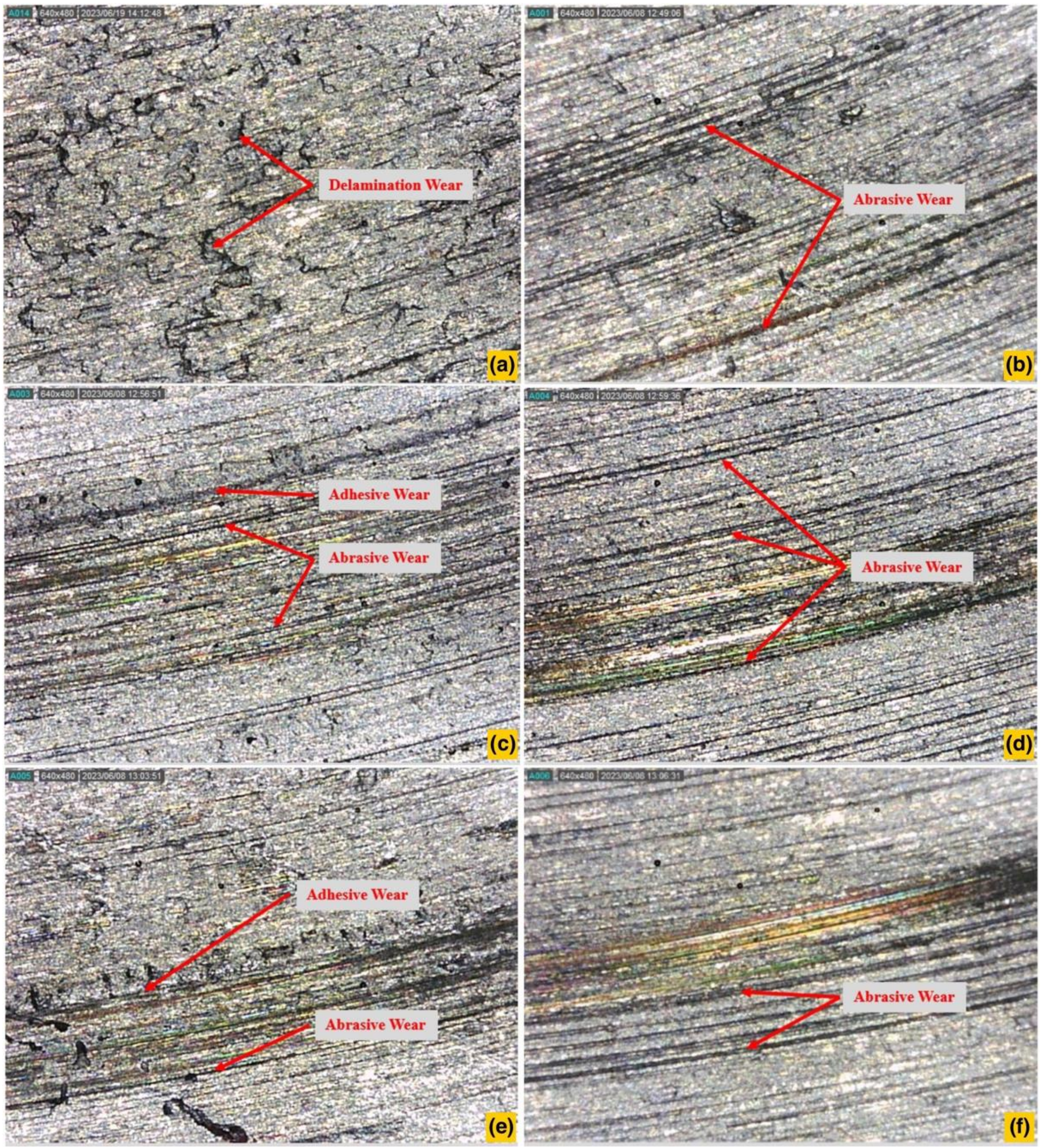


**Figure 14.** Macrostructure of grey cast iron FC25: (a) Dry condition; (b) Base oil A0; (c) Nanolubricant A005; (d) Nanolubricant A010; (e) Nanolubricant A015; (f) Nanolubricant A020

### 3.5.2. Morphology of Grey Cast Iron FC25

**Table 7.** Morphology of grey cast iron FC25

| | Magnification 30X | Magnification 100X |
|---|---|---|
| Dry Condition |  |  |
| A0 |  | 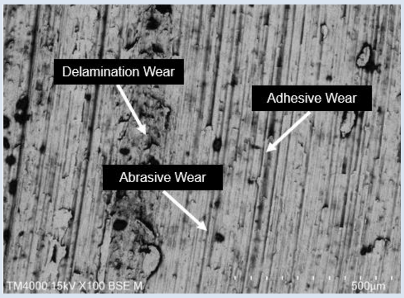 |
| A005 |  | 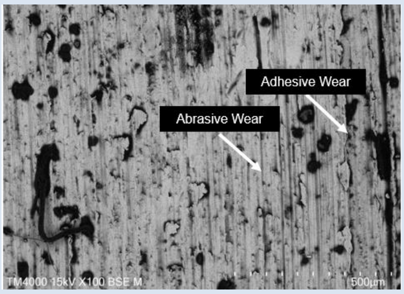 |
| A010 |  | 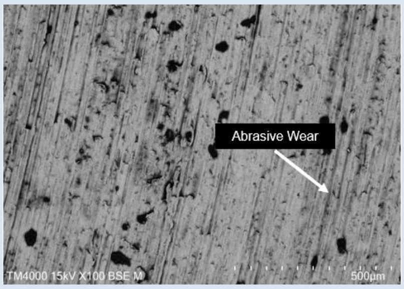 |
| A015 | 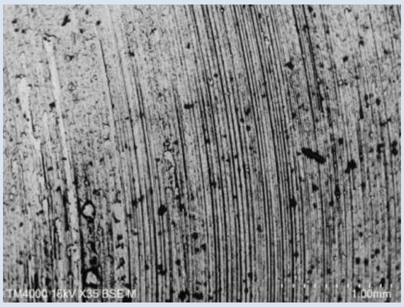 | 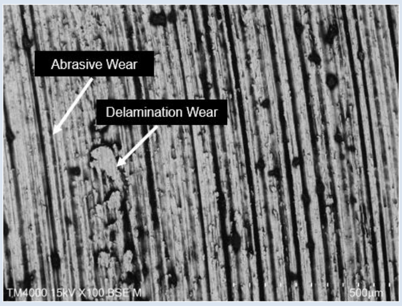 |
| A020 | 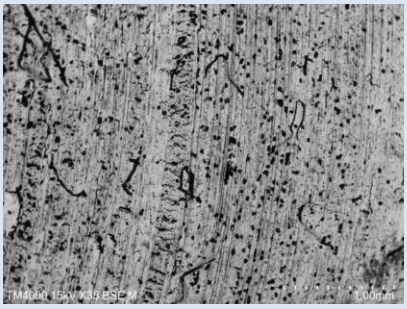 | 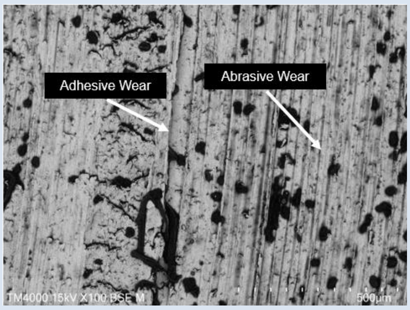 |

In addition to the macrostructure test, the worn surface of the disc was also analyzed through the microstructure using scanning electron microscopy (SEM). This analysis aims to determine the surface morphology of the disc for more apparent results at a certain magnification. The test results are shown in **Table 7** showing that in dry conditions without lubrication, the wear on discs exhibits significant delamination wear, which steadily increases throughout the test duration [61]. The use of SAE 10W-30 base oil reduces wear on the material as there is less direct rubbing of surfaces [62]. Meanwhile, the addition of $CaCO_3$ additive at a concentration of 0.05 wt% and 0.1 wt% in base oil has better wear reduction results compared to base oil. Meanwhile, the addition of $CaCO_3$ additive at 0.15 wt% and 0.2 wt% concentration exhibit higher wear result compared to the base lubricant.

# 4. Conclusion

According to the analysis of the performance of nanolubricant with $CaCO_3$ nanoparticle addition at mass variations of 0.05, 0.15, and 0.2 wt% to enhance wear resistance in FC25 cast iron material, several conclusions have been made. The surface morphology of $CaCO_3$ powder has a round shape and $CaCO_3$ particles have a size of 52.18 nm. The addition of $CaCO_3$ nanoparticles to the base lubricant can increase the wear resistance value as evidenced by the test results. The addition of $CaCO_3$ nanoparticles in base oils can have a good impact on thermophysical properties as evidenced by the test results of thermal conductivity, density, and viscosity which are increasing. The addition of $CaCO_3$ to the base oil also results in a linear flow between the shear rate and shear stress, corresponding with the Newtonian flow. In the nanolubricant performance test, the best COF, mass loss, and surface roughness values of 0.0706, 0.0037 gram, and 0.05 µm are observed from samples with a concentration of 0.1 wt%, respectively. Therefore, the best wear reduction is from nanolubricant with the addition of nano $CaCO_3$ powder additives at 0.1 wt% concentration. It proves that the use of $CaCO_3$ nanoparticles has a good impact on the performance of the nano lubricant.

# Acknowledgements

The authors would like to thank Universitas Negeri Malang for the Dissertation Thesis Grant. Also, thank you to the Department of Mechanical Engineering and Students who helped with this research.

# Authors' Declaration

**Authors' contributions and responsibilities** - The authors made substantial contributions to the conception and design of the study. The authors took responsibility for data analysis, interpretation and discussion of results. The authors read and approved the final manuscript.

**Funding** – This research is funded by the Universitas Negeri Malang for the Dissertation Thesis Grant in 2023 for PP.

**Availability of data and materials** - All data is available from the authors.

**Competing interests** - The authors declare no competing interest.

**Additional information** – No additional information from the authors.

# References

[1] T. W. Agustini, S. E. Ratnawati, B. A. Wibowo, and J. Hutabarat, "Utilization of Clam Amusium Pleuronectes Shell as calcium Source on Extrudates Product," *Jurnal Pengolahan Hasil Perikanan Indonesia*, vol. 14, no. 2, pp. 134–142, 2011.

[2] N. F. Azman and S. Samion, "Dispersion stability and lubrication mechanism of nanolubricants: a review," *International journal of precision engineering and manufacturing-green technology*, vol. 6, pp. 393–414, 2019, doi: 10.1007/s40684-019-00080-x.

[3] J. Basiron, M. Fadzli, B. Abdollah, M. Ilman, and C. Abdullah, "Tribology International Lubricant mechanisms of eco-friendly lubricant blended with mineral oil for steel-steel contact," *Tribology International*, vol. 186, no. April, p. 108653, 2023, doi:

10.1016/j.triboint.2023.108653.

[4] C. H. Chan, S. W. Tang, N. K. Mohd, W. H. Lim, S. K. Yeong, and Z. Idris, "Tribological behavior of biolubricant base stocks and additives," *Renewable and Sustainable Energy Reviews*, vol. 93, no. March 2017, pp. 145–157, 2018, doi: 10.1016/j.rser.2018.05.024.

[5] A. F. Firmansyah, A. I. Gunawan, I. A. Sulistijono, and D. Hanurawan, "Pengukuran Nilai Densitas pada Minyak Pelumas Sepeda Motor dengan Gelombang Ultrasonik," *Jurnal Rekayasa Elektrika*, vol. 18, no. 1, 2022, doi: 10.17529/jre.v18i1.24919.

[6] Y. M. Shashidhara and S. R. Jayaram, "Vegetable oils as a potential cutting fluid-An evolution," *Tribology International*, vol. 43, no. 5–6, pp. 1073–1081, 2010, doi: 10.1016/j.triboint.2009.12.065.

[7] M. S. Gemsprim, N. Babu, and S. Udhayakumar, "Tribological evaluation of vegetable oil-based lubricant blends," *Materials Today: Proceedings*, vol. 37, no. Part 2, pp. 2660–2665, 2020, doi: 10.1016/j.matpr.2020.08.521.

[8] N. N. M. Zawawi, W. H. Azmi, A. A. M. Redhwan, A. I. Ramadhan, and H. M. Ali, "Optimization of Air Conditioning Performance with Al2O3-SiO2/PAG Composite Nanolubricants Using the Response Surface Method," *Lubricants*, vol. 10, no. 10, 2022, doi: 10.3390/lubricants10100243.

[9] M. A. Kumar, A. A. V. P. Rao, and J. H. N. Rao, "Design and Analysis of Dry Cylinder Liners Used in Diesel Engines," *International Journal of Research and Innovative Technology*, vol. 3, no. 9, pp. 518–526, 2015.

[10] L. Gong, S. Qian, W. Wang, Z. Ni, and L. Tang, "Influence of nano-additives (nano-PTFE and nano-CaCO3) on tribological properties of food-grade aluminum-based grease," *Tribology International*, vol. 160, no. March, p. 107014, 2021, doi: 10.1016/j.triboint.2021.107014.

[11] C. GU, Q. LI, Z. GU, and G. ZHU, "Study on application of CeO2 and CaCO3 nanoparticles in lubricating oils," *Journal of Rare Earths*, vol. 26, no. 2, pp. 163–167, 2008, doi: 10.1016/S1002-0721(08)60058-7.

[12] A. Setiawan, F. D. Wahyuningsih, and R. Z. Mirahati, "Mechanical Properties of Biocomposite with Various Composition of CaCO3 and Starch," *Journal of Mechanical Engineering Science and Technology (JMEST)*, vol. 7, no. 1, p. 1, 2023, doi: 10.17977/um016v7i12023001.

[13] K. Vyavhare, R. B. Timmons, A. Erdemir, and P. B. Aswath, "Tribological Interaction of Plasma-Functionalized CaCO3 Nanoparticles with Zinc and Ashless Dithiophosphate Additives," *Tribology Letters*, vol. 69, no. 2, pp. 1–23, 2021, doi: 10.1007/s11249-021-01423-z.

[14] A. S. Al-Janabi, M. Hussin, M. Z. Abdullah, and M. A. Ismail, "Effect of CTAB surfactant on the stability and thermal conductivity of mono and hybrid systems of graphene and FMWCNT nanolubricant," *Colloids and Surfaces A: Physicochemical and Engineering Aspects*, vol. 648, no. May, p. 129275, 2022, doi: 10.1016/j.colsurfa.2022.129275.

[15] Suprapto, T. Sujitno, Taufik, A. Abdussalam, and D. Priyantoro, "Surface Analysis of Ion Nitrided Aluminium Alloy (AlSiCu)," *GANENDRA Majalah IPTEK Nuklir*, vol. 19, no. 2, pp. 65–74, 2016, doi: 10.17146/gnd.2016.19.2.2999.

[16] T. Wopelka *et al.*, "Wear of different material pairings for the cylinder liner – piston ring contact," *Industrial Lubrication and Tribology*, vol. 70, no. 4, pp. 687–699, 2018, doi: 10.1108/ILT-07-2017-0218.

[17] X. Wang, Y. Zhang, Z. Yin, Y. Su, Y. Zhang, and J. Cao, "Experimental research on tribological properties of liquid phase exfoliated graphene as an additive in SAE 10W-30 lubricating oil," *Tribology International*, vol. 135, no. January, pp. 29–37, 2019, doi: 10.1016/j.triboint.2019.02.030.

[18] N. . Nguyen, M. . Chen, S. . Huang, and Y. . Kao, "An experimental method of the cutting force coefficient estimation of grey cast iron FC25," in *International Conference on Applied Mechanics, Materials, and Structural Engineering (ICAMMSE 2015)*, 2016, pp. 192–198.

[19] J. M. Liñeira del Río, A. Alba, M. J. G. Guimarey, J. I. Prado, A. Amigo, and J. Fernández, "Surface tension, wettability and tribological properties of a low viscosity oil using CaCO3 and CeF3 nanoparticles as additives," *Journal of Molecular Liquids*, vol. 391, no. September, 2023, doi: 10.1016/j.molliq.2023.123188.

[20] T. Mahsuli, A. Larasati, A. Aminnudin, and J. Maulana, "Effect of the Homogenization Process on Titanium Oxide-Reinforced Nanocellulose Composite Membranes," *Journal of Mechanical*

*Engineering Science and Technology (JMEST)*, vol. 7, no. 2, p. 137, 2023, doi: 10.17977/um016v7i22023p137.

[21] P. Puspitasari, A. A. Permanasari, M. I. H. C. Abdullah, D. D. Pramono, and O. J. Silaban, “Tribology Characteristic of Ball Bearing SKF RB-12.7/G20W using SAE 5W-30 Lubricant with Carbon-Based Nanomaterial Addition,” *Tribology in Industry*, vol. 45, no. 3, 2023, doi: 10.24874/ti.1538.09.23.11.

[22] Brookfield Engineering Labs. Inc., *More Solutions to Sticky Problems: A Guide to Getting More From Your Brookfield Viscometer*. 2003.

[23] S. K. Kurre, J. Yadav, A. Mudgal, N. Malhotra, A. Shukla, and V. K. Srivastava, “Experimental study of friction and wear characteristics of bio-based lubricant on pin-on-disk tribometer,” *Materials Today: Proceedings*, no. xxxx, 2023, doi: 10.1016/j.matpr.2023.02.071.

[24] R. A. Ningrum, S. Humaidi, S. Sihotang, D. Bonardo, and Estananto, “Synthesis and material characterization of calcium carbonate (CaCO3) from the waste of chicken eggshells,” *Journal of Physics: Conference Series*, vol. 2193, no. 1, 2022, doi: 10.1088/1742-6596/2193/1/012009.

[25] C. Kosanović, S. Fermani, G. Falini, and D. Kralj, “Crystallization of calcium carbonate in alginate and xanthan hydrogels,” *Crystals*, vol. 7, no. 12, pp. 1–15, 2017, doi: 10.3390/cryst7120355.

[26] P. Puspitasari, D. M. Utomo, H. F. N. Zhorifah, A. A. Permanasari, and R. W. Gayatri, “Physicochemical determination of calcium carbonate (CaCO3) from chicken eggshell,” *Key Engineering Materials*, vol. 840 KEM, pp. 478–483, 2020, doi: 10.4028/www.scientific.net/kem.840.478.

[27] S. S. Sanukrishna, S. Vishnu, and M. Jose Prakash, “Experimental investigation on thermal and rheological behaviour of PAG lubricant modified with SiO2 nanoparticles,” *Journal of Molecular Liquids*, vol. 261, pp. 411–422, 2018, doi: 10.1016/j.molliq.2018.04.066.

[28] D. D. Pramono and P. Puspitasari, “Comparison of physicochemical properties of hydroxyapatite from scallop shell synthesized by wet chemical method with and without sonication process,” *AIP Conference Proceedings*, vol. 2991, no. 1, p. 40034, Jun. 2024, doi: 10.1063/5.0199107.

[29] N. S. W. Supriyanto, Sukarni, P. Puspitasari, and A. A. Permanasari, “Synthesis and characterization of CaO/CaCO3 from quail eggshell waste by solid state reaction process,” *AIP Conference Proceedings*, vol. 2120, no. July 2019, 2019, doi: 10.1063/1.5115670.

[30] M. S. Tizo *et al.*, “Efficiency of calcium carbonate from eggshells as an adsorbent for cadmium removal in aqueous solution,” *Sustainable Environment Research*, vol. 28, no. 6, pp. 326–332, 2018, doi: 10.1016/j.serj.2018.09.002.

[31] P. Kamalanathan *et al.*, “Synthesis and sintering of hydroxyapatite derived from eggshells as a calcium precursor,” *Ceramics International*, vol. 40, no. PB, pp. 16349–16359, 2014, doi: 10.1016/j.ceramint.2014.07.074.

[32] M. Ding and N. Ni, “Preparation and characterization of biomorphic CaCO3 with hierarchically ordered micro-and nano-structures,” *Asian Journal of Chemistry*, vol. 25, no. 10, pp. 5652–5654, 2013, doi: 10.14233/ajchem.2013.oh50.

[33] Y. Wei *et al.*, “Synthesis and characterization of porous CaCO3 microspheres templated by yeast cells and the application as pH value-sensitive anticancer drug carrier,” *Colloids and Surfaces B: Biointerfaces*, vol. 199, no. September 2020, p. 111545, 2021, doi: 10.1016/j.colsurfb.2020.111545.

[34] Z. Yang, Y. Tang, and J. Zhang, “Surface modification of CaCO3 nanoparticles with silane coupling agent for improvement of the interfacial compatibility with styrene-butadiene rubber (SBR) latex,” *Chalcogenide Letters*, vol. 10, no. 4, pp. 131–141, 2013.

[35] K. Apmann, R. Fulmer, A. Soto, and S. Vafaei, “Thermal conductivity and viscosity: Review and optimization of effects of nanoparticles,” *Materials*, vol. 14, no. 5, pp. 1–75, 2021, doi: 10.3390/ma14051291.

[36] H. Ebadi-Dehaghani, M. Reiszadeh, A. Chavoshi, M. Nazempour, and M. H. Vakili, “The effect of zinc oxide and calcium carbonate nanoparticles on the thermal conductivity of polypropylene,” *Journal of Macromolecular Science, Part B: Physics*, vol. 53, no. 1, pp. 93–107, 2013, doi: 10.1080/00222348.2013.810032.

[37] M. A. B. Saufi and H. B. Mamat, “A Review on Thermophysical Properties for Heat Transfer

Enhancement of Carbon-Based Nanolubricant," *Advanced Engineering Materials*, vol. 23, no. 10, pp. 1–20, 2021, doi: 10.1002/adem.202100403.

[38] M. Gupta, V. Singh, R. Kumar, and Z. Said, "A review on thermophysical properties of nanofluids and heat transfer applications," *Renewable and Sustainable Energy Reviews*, vol. 74, no. December 2015, pp. 638–670, 2017, doi: 10.1016/j.rser.2017.02.073.

[39] Y. Mahshuri, M. A. Amalina, and C. A. Nurnadhiah Nadhirah, "Thermal conductivity of calcium carbonate filled with unsaturated polyester composites with different filler sizes," *Materials Research Innovations*, vol. 18, pp. S6-340-S6-344, 2014, doi: 10.1179/1432891714Z.0000000001023.

[40] P. A. C. Gane, C. J. Ridgway, J. Schoelkopf, and D. W. Bousfield, "Heat transfer through calcium carbonate-based coating structures: Observation and model for a thermal fusing process," *Journal of Pulp and Paper Science*, vol. 33, no. 2, pp. 60–70, 2014.

[41] H. Mamat, "Nanofluids: Thermal Conductivity and Applications," *Reference Module in Materials Science and Materials Engineering*, 2019, doi: 10.1016/b978-0-12-803581-8.11569-3.

[42] A. I. Ramadhan, W. H. Azmi, E. Umar, and A. M. Sari, "Heat transfer performance of Al2O3-TiO2-SiO2 ternary nanofluids in plain tube with wire coil inserts," *Mechanical Engineering for Society and Industry*, vol. 4, no. 1, pp. 50–67, 2024, doi: 10.31603/mesi.10996.

[43] E. V. Timofeeva, W. Yu, D. M. France, D. Singh, and J. L. Routbort, "Nanofluids for heat transfer: An engineering approach," *Nanoscale Research Letters*, vol. 6, no. 1, pp. 1–7, 2011, doi: 10.1186/1556-276X-6-182.

[44] H. Babar and H. M. Ali, "Towards hybrid nanofluids: Preparation, thermophysical properties, applications, and challenges," *Journal of Molecular Liquids*, vol. 281, pp. 598–633, 2019, doi: 10.1016/j.molliq.2019.02.102.

[45] K. Elsaid *et al.*, "Thermophysical properties of graphene-based nanofluids," *International Journal of Thermofluids*, vol. 10, 2021, doi: 10.1016/j.ijft.2021.100073.

[46] M. F. Nabil, W. H. Azmi, K. A. Hamid, and R. Mamat, "Experimental investigation of heat transfer and friction factor of TiO2-SiO2 nanofluids in water:ethylene glycol mixture," *International Journal of Heat and Mass Transfer*, vol. 124, pp. 1361–1369, 2018, doi: 10.1016/j.ijheatmasstransfer.2018.04.143.

[47] A. Dhanola and H. C. Garg, "Experimental analysis on stability and rheological behaviour of TiO2/canola oil nanolubricants," *Materials Today: Proceedings*, vol. 28, pp. 1285–1289, 2020, doi: 10.1016/j.matpr.2020.04.245.

[48] P. Puspitasari, A. A. Permanasari, M. S. Shaharun, and D. I. Tsamroh, "Heat transfer characteristics of NiO nanofluid in heat exchanger," *AIP Conference Proceedings*, vol. 2228, no. April, 2020, doi: 10.1063/5.0000883.

[49] S. A. Angayarkanni and J. Philip, "Review on thermal properties of nanofluids: Recent developments," *Advances in Colloid and Interface Science*, vol. 225, pp. 146–176, 2015, doi: 10.1016/j.cis.2015.08.014.

[50] L. Yang, W. Ji, M. Mao, and J. nan Huang, "An updated review on the properties, fabrication and application of hybrid-nanofluids along with their environmental effects," *Journal of Cleaner Production*, vol. 257, p. 120408, 2020, doi: 10.1016/j.jclepro.2020.120408.

[51] Safril, W. H. Azmi, N. N. M. Zawawi, and A. I. Ramadhan, "Tribology Performance of TiO2-SiO2/PVE Nanolubricant at Various Binary Ratios for the Automotive Air-conditioning System," *Automotive Experiences*, vol. 6, no. 3, pp. 485–496, 2023, doi: 10.31603/ae.10255.

[52] M. H. Aghahadi, M. Niknejadi, and D. Toghraie, "An experimental study on the rheological behavior of hybrid Tungsten oxide (WO3)-MWCNTs/engine oil Newtonian nanofluids," *Journal of Molecular Structure*, vol. 1197, pp. 497–507, 2019, doi: 10.1016/j.molstruc.2019.07.080.

[53] M. H. Esfe, S. Saedodin, and J. Shahram, "Experimental investigation, model development and sensitivity analysis of rheological behavior of ZnO/10W40 nano-lubricants for automotive applications," *Physica E: Low-Dimensional Systems and Nanostructures*, vol. 90, no. February, pp. 194–203, 2017, doi: 10.1016/j.physe.2017.02.015.

[54] R. Thirugnanasambantham, T. Elango, and K. Elangovan, "Wear and friction characterization of chlorella sp. Microalgae oil based blended lubricant on pin on disc tribometer," *Materials*

*Today: Proceedings*, vol. 33, pp. 3063–3067, 2020, doi: 10.1016/j.matpr.2020.03.512.

[55] A. Kader, V. Selvaraj, P. Ramasamy, and K. Senthilkumar, “Experimental investigation on the thermo-physical properties and tribological performance of acidic functionalized graphene dispersed VG-68 hydraulic oil-based nanolubricant,” *Diamond and Related Materials*, vol. 133, no. September 2022, p. 109740, 2023, doi: 10.1016/j.diamond.2023.109740.

[56] D. F. M. Pico, L. R. R. da Silva, O. S. H. Mendoza, and E. P. Bandarra Filho, “Experimental study on thermal and tribological performance of diamond nanolubricants applied to a refrigeration system using R32,” *International Journal of Heat and Mass Transfer*, vol. 152, p. 119493, 2020, doi: 10.1016/j.ijheatmasstransfer.2020.119493.

[57] M. Sepehrnia, H. Maleki, and M. F. Behbahani, “Tribological and rheological properties of novel MoO3-GO-MWCNTs/5W30 ternary hybrid nanolubricant: Experimental measurement, development of practical correlation, and artificial intelligence modeling,” *Powder Technology*, vol. 421, no. January, p. 118389, 2023, doi: 10.1016/j.powtec.2023.118389.

[58] M. Mosleh, N. D. Atnafu, J. H. Belk, and O. M. Nobles, “Modification of sheet metal forming fluids with dispersed nanoparticles for improved lubrication,” *Wear*, vol. 267, no. 5–8, pp. 1220–1225, 2009, doi: 10.1016/j.wear.2008.12.074.

[59] A. Amanov, B. Ahn, M. G. Lee, Y. Jeon, and Y. S. Pyun, “Friction and wear reduction of eccentric journal bearing made of sn-based babbitt for ore cone crusher,” *Materials*, vol. 9, no. 11, 2016, doi: 10.3390/ma9110950.

[60] A. Amanov, Y. S. Pyun, and S. Sasaki, “Effects of ultrasonic nanocrystalline surface modification (UNSM) technique on the tribological behavior of sintered Cu-based alloy,” *Tribology International*, vol. 72, pp. 187–197, 2014, doi: 10.1016/j.triboint.2013.12.003.

[61] H. Yang *et al.*, “The formation of the delamination wear of the pure carbon strip and its influence on the friction and wear properties of the pantograph and catenary system,” *Wear*, vol. 454–455, no. 4, 2020, doi: 10.1016/j.wear.2020.203343.

[62] P. Puspitasari, A. A. Permanasari, A. Warestu, G. P. P. Arifiansyah, D. D. Pramono, and T. Pasang, “Tribology Properties on 5W-30 Synthetic Oil with Surfactant and Nanomaterial Oxide Addition,” *Automotive Experiences*, vol. 6, no. 3, pp. 669–686, 2023, doi: 10.31603/ae.10115.